

# Combination of $\mu$ GISAXS and imaging ellipsometry at the MiNaXS instrument at PETRA III

V. Körstgens, M. Rawolle, A. Buffet<sup>1</sup>, R. Döhrmann<sup>1</sup>, K. Stassig<sup>1</sup>, S.V. Roth<sup>1</sup>, and P. Müller-Buschbaum

Technische Universität München, Lehrstuhl für Funktionelle Materialien, Physik-Department E13, James-Franck-Str. 1, D-85747 Garching, Germany

<sup>1</sup> HASYLAB at DESY, Notkestraße 85, D-22607 Hamburg, Germany

The possibilities of the surface sensitive scattering method grazing incidence small angle x-ray scattering (GISAXS) were expanded by the integration of in-situ imaging ellipsometry recently [1]. In autumn 2010 we were able to install for the first time the combined instrument at the micro- and nanofocus x-ray scattering beamline (MiNaXS/P03) at the synchrotron source PETRA III.

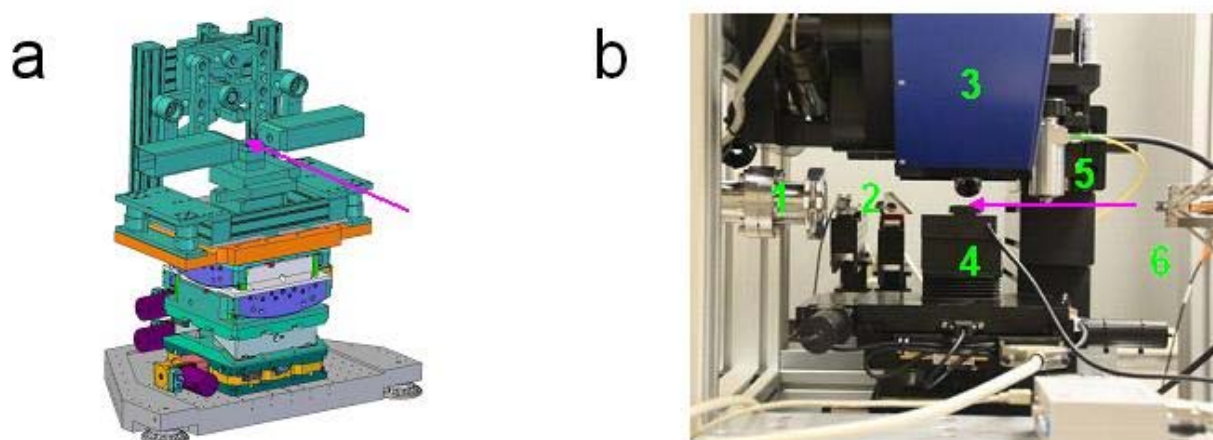


**Figure 1:** Ellipsometer installation at beamline MiNaXS **a:** Sketch of imaging ellipsometer mounted on positioning system **b:** sample environment with 1: entrance window of flight tube towards detector, 2: beamstops for direct beam, 3: laser arm of ellipsometer, 4: sample stage of ellipsometer, 5: AFM, 6: guard slits; the arrows show the direction of the x-ray beam from the source.

The imaging ellipsometer SPEM, a single wavelength (532 nm) instrument, of Nanofilm Technologie GmbH, was installed at the beamline MiNaXS as shown in figure 1. The concept of the combined instrument is that the sample is placed horizontally (xy plane) on the alignment stage of the ellipsometer. After ellipsometric alignment and measurement with a lateral resolution of 1  $\mu\text{m}$  the desired incidence angle for the x-ray beam is set by tilting the whole ellipsometer set-up. The whole stack of positioning stages including 2-circle segment is mounted on a base, which can be moved in the experimental hutch by air pads. It is depicted in figure 1a. A singular calibration of the instrument is necessary to ensure that the laser beam and the x-ray beam cross each other at one known point on the sample surface. In figure 2 an in-situ measurement of a thin films of polymer material especially sensitive to x-ray radiation damage, as used for calibration, is shown. The field of view of the imaging ellipsometer depends on the angle of incidence of the laser beam and the objective chosen. For an angle of  $55^\circ$  and an objective with 20x magnification a field of view of  $201 \mu\text{m} \times 263 \mu\text{m}$  develops. With three different assigned regions of interest (ROIs)(figure 2a) the course of  $\Delta$  and  $\Psi$  averaged over every pixel of the according ROI can be followed as the x-ray beam illuminates the surface. Due to the sensitive sample an instantaneous change in  $\Delta$  and  $\Psi$  for the central ROI with switching on the x-ray beam is shown in figure 2c with open circles. If x-ray illumination is stopped  $\Delta$  and  $\Psi$  immediately show constant values. The width of the foot print visible live in the field of view during x-ray illumination, shown in figure 2b, corresponds to the beamsizes of  $35 \mu\text{m} \times 22 \mu\text{m}$  used in this experiment. An alternative to the acquisition of  $\Delta$  and  $\Psi$  in chosen ROIs is the recording of 2d images in the full field of view ( $\Delta$  and  $\Psi$  -maps) [1].

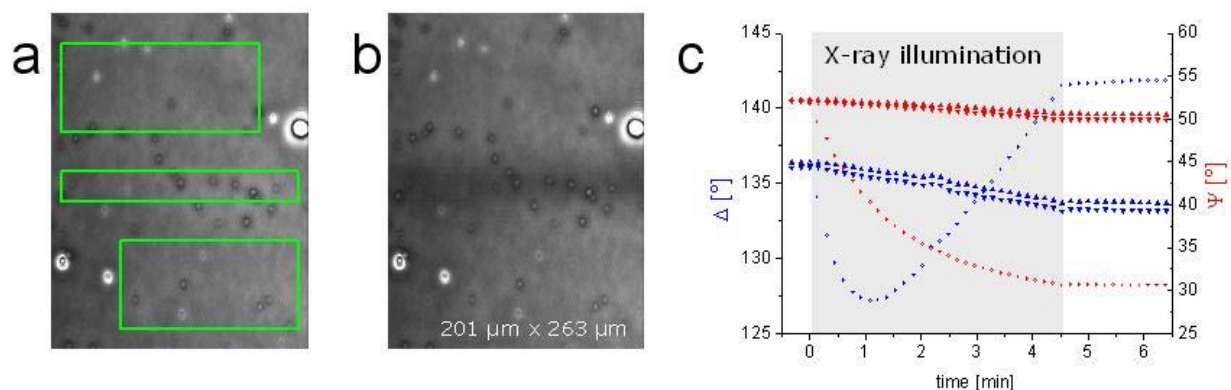


**Figure 2:** Measurement of calibration sample **a:** field of view of imaging ellipsometer with three chosen regions of interests (ROIs, green line) **b:** visible footprint of x-ray beam due to x-ray illumination **c** course of ellipsometric values  $\Delta$  and  $\Psi$  in ROIs during illumination with x-ray beam; open symbols: central ROI.

The combination of  $\mu$ GISAXS and imaging ellipsometry is particularly suited for the investigation of kinetic processes. As an example given in figure 3, the drying of a droplet of gold nanorods in aqueous dispersion along a gradient of polydimethylsiloxane (PDMS) on silicon substrate is followed. The values of  $\Delta$  and  $\Psi$  are recorded in three different ROIs (figure 3a) analogue to the measurement of the calibration sample described above. The corresponding 2d GISAXS scattering patterns counted for 2 s are shown in figure 3b (time since start of data acquisition is indicated). After 6 s the scattering pattern corresponds to the sample surface before droplet deposition. With droplet deposition there is an immediate change in  $\Delta$  and  $\Psi$  (figure 3a). The corresponding scattering intensity (figure 3b: 100 s) is very low in comparison to the substrate before droplet deposition. Only weak intensity is displayed on the detector because the large droplet volume absorbs strongly the transmitting x-ray beam.

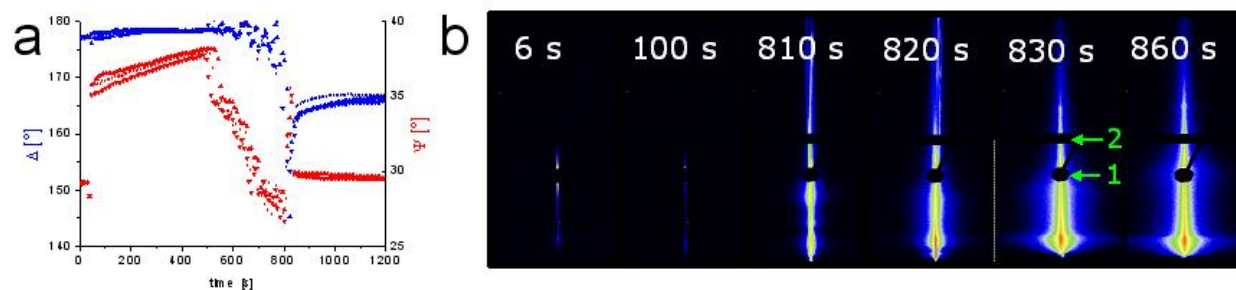


**Figure 3:** In situ experiment of a drying droplet of gold nanorod dispersion **a:** course of ellipsometric values  $\Delta$  and  $\Psi$  in different ROIs **b:** detail of 2D GISAXS pattern with time; 1: specular beamstop; 2: frame bordering modules of Pilatus detector.

The arrangement of nanorods on the surface is evident not before 810 s, when the scattering pattern with much higher intensity evolves (figure 3b: 810 s). Notably, for the duration of the drying experiment the  $\Delta$  and  $\Psi$  values shown in figure 3a at any given time are similar for all three chosen ROIs. In case of severe damage of the sample due to the high brilliance x-ray beam  $\Delta$  and  $\Psi$  values would differ over time for the ROIs in- and outside the footprint of the x-ray beam as shown in figure 2c.

This work has been financially supported by the BMBF (grant number 05KS7WO1).

## References

- [1] V. Körstgens, J. Wiedersich, R. Meier, J. Perlich, S.V. Roth, R. Gehrke and P. Müller-Buschbaum, *Anal. Bioanal. Chem.* **396**, 139 (2010).